

Study of Multicast Broadcast Single Frequency Network Area in Multicast Communication

Chen Shen^{*†}, Chunmei Liu[‡], Richard A. Rouil[‡], and Hyeong-Ah Choi[§]

^{*}Associate, Wireless Networks Division, National Institute of Standards and Technology, USA

[†]Department of Physics, Georgetown University, USA

[‡]Wireless Networks Division, National Institute of Standards and Technology, USA

[§]Department of Computer Science, George Washington University, USA

Email: [†]sc1951@georgetown.edu [‡]{chunmei.liu, richard.rouil}@nist.gov, [§]hchoi@gwu.edu

Abstract—Multicast was introduced in Long-Term Evolution (LTE) in release 8 as the technology for the Evolved Multimedia Broadcast Multicast Services (eMBMS) and has been steadily updated in the later releases. Unlike unicast where available resources are split amongst each User Equipment (UE), in Multicast Broadcast Single Frequency Network (MBSFN), all the resources can be allocated to reach all UEs. This prominent advantage together with the prevalent signal improvement make MBSFN a popular LTE and 5G evolution technique. In this paper, we focus on the LTE Multicast Broadcast Single Frequency Network (MBSFN) technology from the perspective of the MBSFN area and its application in public safety networks (PSNs). Since the MBSFN area plays a pivotal role in performance improvement and public safety incidents differ in their scales, using our state-of-the-art system-level simulations, we explore performance distributions within MBSFN areas of different shapes and sizes, as well as the impacts of MBSFN area locations relative to the network. We show that the results can give an informative insight into the MBSFN area for in-coverage performance prediction/evaluation or out-of-coverage mobile base station deployments.

Index Terms—LTE, MBSFN area, resource efficiency.

I. INTRODUCTION

While the majority of Long-Term Evolution (LTE) downlink transmissions uses unicast to achieve excellent performance, when transmitting the same content to a large group of User Equipment (UEs), LTE Multicast Broadcast Single Frequency Network (MBSFN) shows excellent potential performance improvement over unicast [1]. To serve this type of traffic, in unicast, available resources are split into sets of resource blocks (RBs) and each UE gets its own share. The content is then mapped to each RB set and transmitted to individual UEs separately. Whereas in MBSFN, multiple cells are configured to form an MBSFN area and tightly synchronized. These cells map the content to the entire available resources and transmit identical waveforms together to all the UEs. From UE perspective, this is equivalent to that each individual UE has full access to the entire available resources. Consequently, in theory, MBSFN can serve an unlimited number of UEs simultaneously, and hence, it can boost the spectral efficiency significantly when serving an enormous number of users [2]. For this reason, MBSFN is of particular interest in public safety communications due to their significant group traffic with a multicast nature.

Supporting multicast transmissions in MBSFN has some limitations. First, spatial multiplexing technology, which plays

an essential role in high LTE unicast performance, is not supported in MBSFN. Next, the current MBSFN protocol lacks the transmission acknowledgments from each UE. To get reliable transmissions, a more conservative Modulation and Coding Scheme (MCS) or Channel Quality Indicator (CQI) is preferred [3] and is combined with a stricter target Block Error Rate (BLER), which is usually 0.01 compared with 0.1 in unicast [4]. Besides, in early LTE releases, the number of subframes allowed for MBSFN is limited to 6 out of 10. This constraint is relaxed in later releases. Furthermore, due to the larger serving size of the MBSFN area, longer Cyclic Prefix (CP) is required. With more reference signals required, the resulting larger overhead leads to much fewer physical resources available for data in each frame, compared with unicast [5].

Last but not least, all UEs served by MBSFN must use the same MCS, which is typically selected to be the minimum of all UEs' to guarantee proper demodulation and decoding [6]. For instance, if the minimum MCS index of all UEs in one MBSFN area is 8, then MCS 8 will be applied to all despite some UEs being able to use higher MCS. In LTE release 15 Table 7.1.7.1-1 [7], MCS index values are defined from 0 to 31, with higher values having higher spectral efficiency.

Despite the above limitations, MBSFN can still outperform unicast in some cases by allowing each UE full access to the entire available resources and by Signal-to-Interference-plus-Noise Ratio (SINR) improvement. Both factors can hardly be quantified for general cases. The first one, full access to the entire available resources, plays a primary role in MBSFN. The more UEs, the higher the spectral efficiency. The only drawback of increasing the UE size is the potential lower MCS for MBSFN, given that the minimum MCS among UEs will be chosen. The second one, SINR improvement, comes from two sources: less inter-cell interference and constructive signal combination from MBSFN cells, which have been analyzed in detail in [8]. In principle, the UE locations relative to the MBSFN area determine the distribution of useful signals and interference, thus different SINR improvement and the resulting performance across the MBSFN area.

This difference in performance across MBSFN areas is not of particular importance in commercial multicast/broadcast due to their large geographic area and that most UEs are at the center. Hence there are little such studies in the literature.

However, the areas covered by public safety incidents differ in size and shape, leading to significant performance differences.

With this in mind, in this paper, we investigate the impact of the MBSFN area and UE locations on the performance with various MBSFN deployment scenarios by using our cutting edge system-level simulations, which take into account all the MBSFN factors mentioned above [9]. When macro-cells are in place in the public safety incident area, our results can give precise performance prediction; For areas without underlying macro-cells, our results can provide guidelines to deploy mobile base stations to serve public safety traffic for various scenarios [10] [11]. To our knowledge, this work is the first of its kind for the MBSFN areas of different schemes with extensive simulation results.

The rest of the paper is organized as follows. In Section II, we briefly describe our system-level simulation and some necessary configurations for the MBSFN settings. In Section III, we present and analyze our simulation results for different MBSFN deployment scenarios. At last, we summarize our observations in Section IV.

II. SYSTEM SIMULATION CONFIGURATIONS FOR MBSFN

In typical non-Coordinated Multi-Point (non-COMP) unicast transmissions, each UE is served by one cell, and the coordination between neighboring cells is limited mainly for interference reduction and handovers. Whereas in MBSFN transmissions, several MBSFN cells form an MBSFN area where UEs inside the area can be served by all the corresponding MBSFN cells. Since the transmitting signals come from several cells, the UEs' positions relative to the area, together with the MBSFN area size and shape, will influence the performance. To explore this impact, we design multiple scenarios for unicast and MBSFN transmissions with different area sizes and shapes.

First, we set the basic scenario of hexagonally distributed three rings of cells for both unicast and MBSFN, as in Figure 1. The red dots with black triangles represent tilted tri-sector sites, each of which counts for three cells. The outer two rings of cells are only to generate interference, and we are only interested in the performance of the central 21 cells (7 tri-sector sites), colored in grey and blue in Figure 1. The antenna configuration for the downlink is eight transmitters and four receivers for both unicast and MBSFN, and transmit mode (TM) 9 is used for the unicast. The simulation length in both cases is 1 second, which counts for 1000 subframes or TTIs (Transmission Time Interval) in the simulations. We also assume zero feedback delay and perfect channel knowledge for the modeling and simulations.

In unicast, due to the symmetricity of the network layout and to reduce the simulation time, we further shrink the area of focus from 21 cells to 7 cells, colored in blue in Figure 1. The different transparencies in the figure indicate the different cell areas.

The largest MBSFN area in our design consists of the central 21 cells, as shown in Figure 2, where the numbers from 1 to 21 indicate the cell indices. The areas colored with

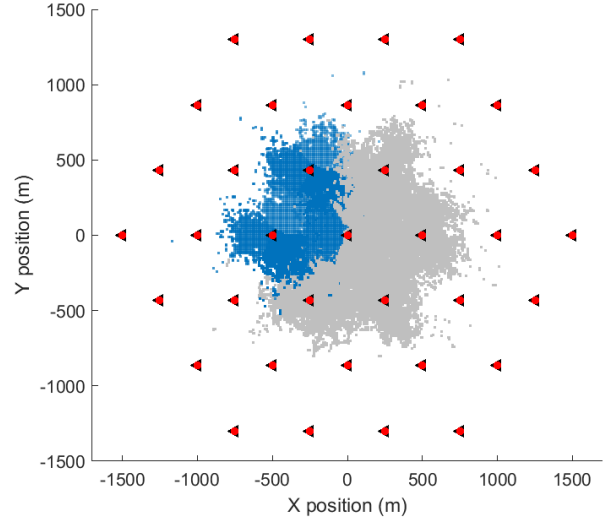


Fig. 1: UE Saturated in 21 and 7 Cells, Respectively

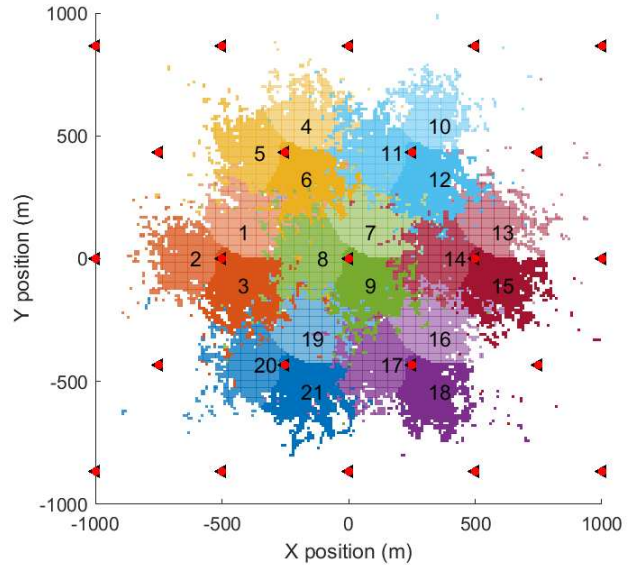


Fig. 2: Network Layout

different transparencies, but the same hue represents three cells of one site. For MBSFN, the performance gain mainly comes from three parts: full physical layer resources for all UEs, the signal combination from all MBSFN cells, and the possible interference reduction from neighboring cells. The latter two gains depend on the MBSFN area's topology but are still centrosymmetric in the basic scenario. Thus we only consider UEs in the selected seven cells (Cell IDs 1 to 8 except 7) as discussed before. It can be seen that this setting extensively reduces simulation computations yet covers UEs at the center, middle, and edge all over the MBSFN area.

Figure 3 further illustrates the constructive signals contributed by multiple cells in the MBSFN area, represented

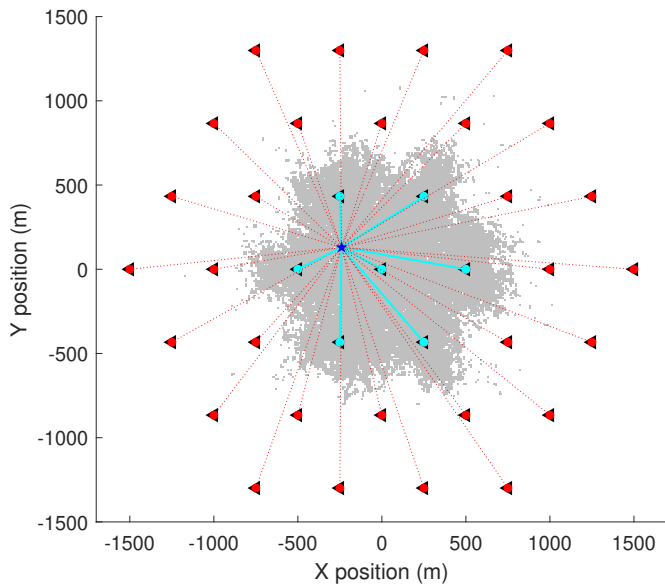


Fig. 3: MBSFN: Signal and Interference

by the solid cyan lines, and the interference from the outer two rings, represented by the dashed red lines. The signals from the cells inside the MBSFN area can also lead to intersymbol interference if it surpasses the extended CP, which is used for MBSFN in our simulations. A detailed analysis has been given in the work [8]. The varieties of network layouts and the signal combination from multiple locations make it too complicated for conventional performance analysis. Therefore, we seek simulations to provide insights into the performance in the designed scenarios.

III. PERFORMANCE ANALYSIS OVER MBSFN AREA AND UE LOCATIONS

A. Wide-band Signal and Interference Comparison

Due to the multi-cell signal combination and interference reduction effect, the wide-band signal and interference can give us a more straightforward picture of the MBSFN behaviors. The signal power in dBm (decibels (dB) with reference to one milliwatt) for MBSFN and unicast are shown in Figure 4 and Figure 5, respectively. Overall, they share a very similar pattern with minor higher values for MBSFN, which is contributed by the signal combination from the 21 MBSFN cells.

Contrary to the signal power, the interference level differs significantly between unicast and MBSFN, as shown in Figure 6 and Figure 7. In unicast, the structure of the individual sites is recognizable, whereas in MBSFN the interference obliterates this pattern and leads to one common center. This is because the MBSFN cells are no longer generating interference to neighbor MBSFN cells, especially at cell edges.

In addition to the interference pattern's shift, the values of the interference level improve tremendously in MBSFN. For the total of 15 058 simulated points in Figure 6 and Figure 7, the mean of interference is reduced from -33.76 dBm

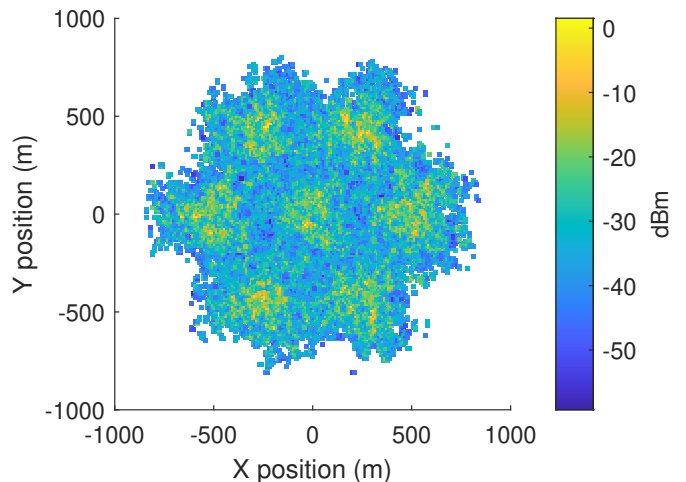


Fig. 4: Unicast: Wide-band Signal

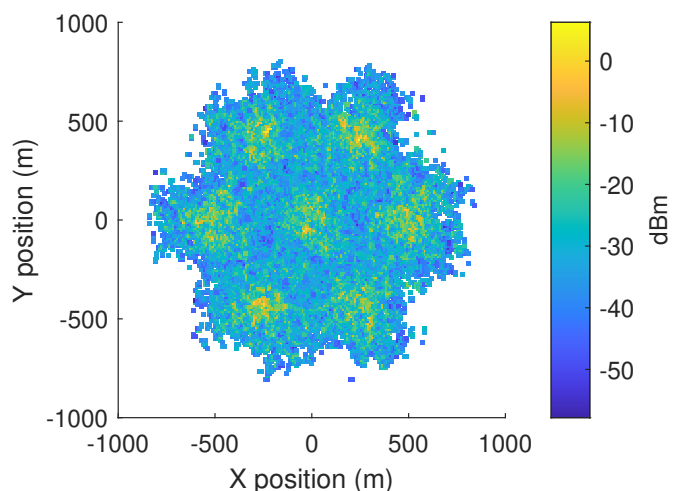


Fig. 5: MBSFN: Wide-band Signal

in unicast to -39.98 dBm in MBSFN, with 95% confidence interval of $[-33.88, -33.65]$ and $[-40.09, -39.87]$ respectively; and the maximum of interference is reduced from 4.53 dBm to -11.84 dBm. These numbers imply that the interference reduction from neighboring cells in MBSFN could improve the UEs' SINR, especially at the center of the MBSFN area. In the majority of locations, this improvement outweighs the improvement from the signal combination discussed previously.

B. Unicast Performance in the Selected Cells

In unicast transmissions, we assume there is no cooperation or CoMP among cells. The performance of different cells should hence be similar. We present the results for this scenario in this section and use them as a benchmark for MBSFN comparisons in the next section. In this study, UEs are dropped at every pixel in the selected seven cells (Figure 1). Table I lists number of UEs dropped at each cell.

Since in multicast, only one single layer is supported in LTE, for fair comparisons, in unicast, we represent the signal portion by single-layer effective post-equalization (SLEPE)

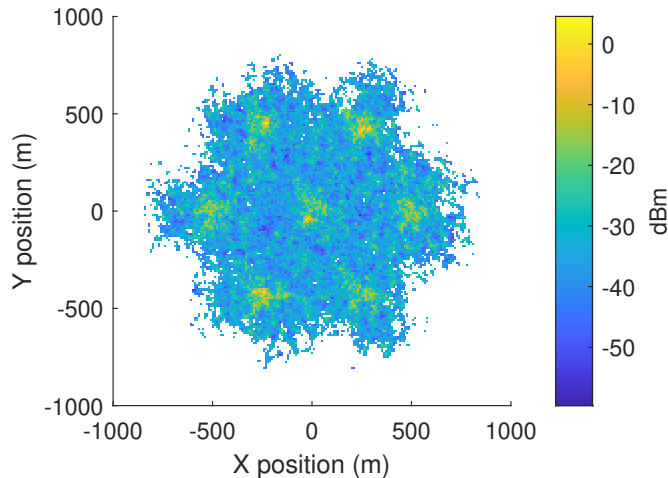


Fig. 6: Unicast: Wide-band Interference

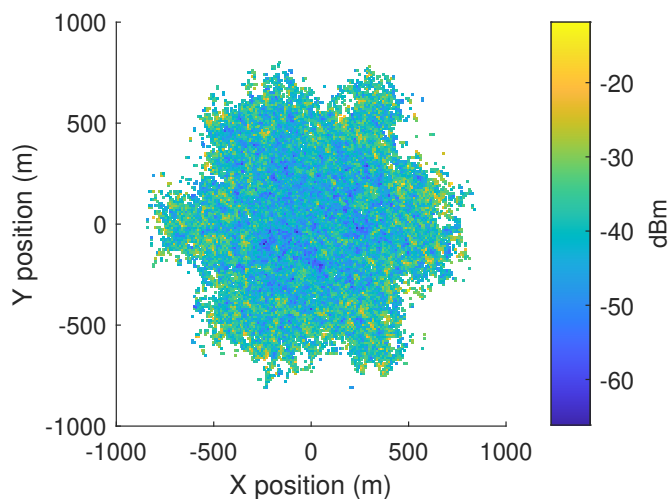


Fig. 7: MBSFN: Wide-band Interference

TABLE I: Cell Size by the Number of UEs

Cell	1	2	3	4	5	6	8
Number of UEs	683	697	820	700	660	735	770

SINR, which is calculated based on the Mutual Information Effective SINR Mapping (MIESM) method [12]. For each UE, we calculate the average SLEPE SINR over time by its arithmetic mean. The Cumulative Distribution Function (CDF) plot is shown in Figure 8. Combined with the number of UEs in each cell as in Table I, it can be seen that the distributions of the unicast UE SINR are quite similar among these cells. This result confirms that unicast cells with similar channel and pathloss models offer comparable performances. Figure 9 further captures the heatmap of the UE SLEPE SINR. It clearly shows the tri-sector site pattern, and that all cells share similar SINR distributions location-wise.

C. MBSFN Performance in the Selected Cells

In the case of MBSFN, the post-equalization SINR averaged over time for each UE in the seven selected cells are shown

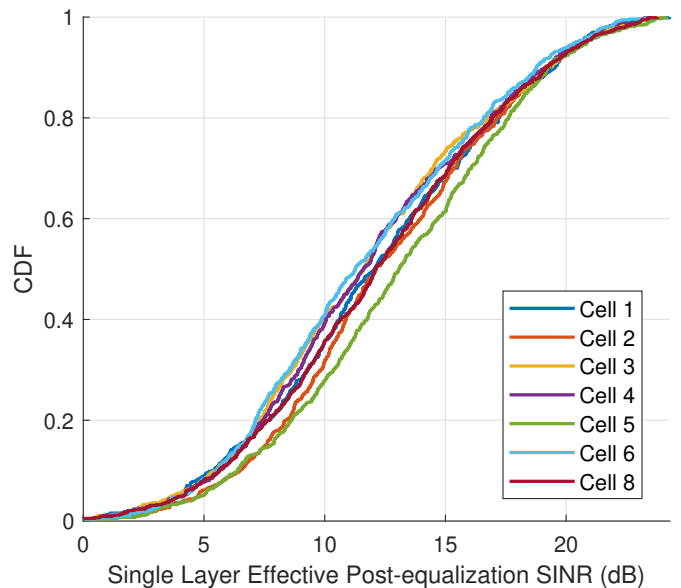


Fig. 8: Unicast: UE Single Layer Effective Post-equalization SINR (dB)

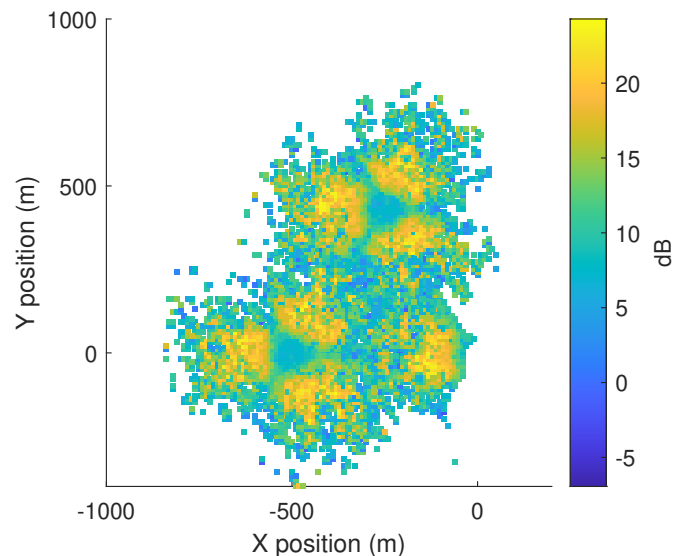


Fig. 9: Unicast: UE SINR Heatmap

in Figure 10. Compared with unicast in Figure 8, UEs in all of the selected cells have significant SINR improvements. For instance, the median SINR in unicast is around 12 dB, while the 25 percentile of SINR in MBSFN is already above 15 dB. This is due to the significant MBSFN gain discussed earlier. One thing to note is that, in reality, further improvement of SINR above a certain threshold has no contribution to the real performance. This is because MBSFN can only use a single data stream, and the maximum MCS caps the required SINR. This threshold is approximately 25 dB in our simulation [13]. For the same reason, only SINR below 30 dB is shown in Figure 10 for MBSFN.

Also, it can be observed that there are more performance

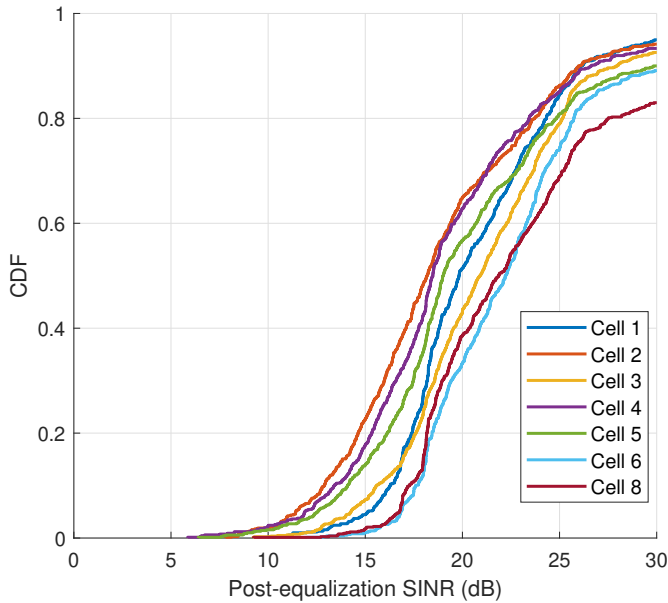


Fig. 10: MBSFN: UE Post-equalization SINR (dB)

variations among cells in MBSFN than in unicast. Some cells have a constant performance advantage over other cells. For example, the SINR in Cell 8 has approximately 4 dB improvement over Cell 2 and Cell 4. From Figure 2, Cell 8 is at the center of the MBSFN area, while Cell 2 and 4 are at the edge. That is, the MBSFN gain decreases from the MBSFN center to the edge. This conclusion can be further verified by the other cells. For example, if we sort the seven cells by how close it is to the center of the MBSFN area visually, we should get the order: 8, 6, 3, 1, 5, 4, and 2 (Cell Index). This order is consistent with the order of SINR CDF curves in Figure 10. This is because the MBSFN area center is further away from interference sources outside the MBSFN area (the outer rings), and at the same time, receives stronger constructive signals within the MBSFN area.

Also, the tri-sector pattern that exists in unicast is weakened in the case of MBSFN because of the different signal and interference distributions, as shown in subsection III-A, which draws an essential difference from the unicast.

D. Other MBSFN Deployment Scenarios

To further explore the impact of the MBSFN area, we analyze different MBSFN area sizes and deployment shapes in terms of the post-equalization SINR. Instead of the 21-cell MBSFN configuration used above, the MBSFN areas in this sub-section are as follows.

First, we introduce two cases with 3-cell MBSFN, whose area consists of 3 MBSFN cells but in different deployment shapes. Case 1 shown in Figure 12a has 3 cells of one site for the MBSFN area, whereas case 2 shown in Figure 14a has 3 cells from 3 different sites that make up the MBSFN area. Both cases share the same area shape and number of cells but differ in cell radiation directional pattern. If we set a cell with a radiation direction, case 1 is centrifugal, whereas case 2 is similar to centripetal.

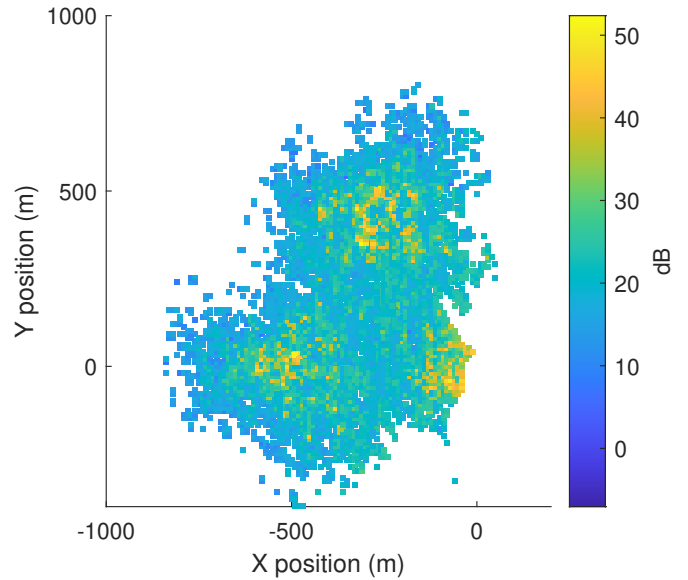


Fig. 11: MBSFN: UE SINR Heatmap

The post-equalization SINR in these 2 cases have very distinctive distributions, as shown in the SINR heatmaps in Figure 12b and Figure 14b, as well as the SINR CDFs in Figure 13 and Figure 15. We can observe that case 1 SINR has a concentric hierarchy pattern, while it is more evenly distributed in case 2. The maximum SINR in case 1 can reach 45 dB, accompanied by a significant SINR portion below 15 dB. In contrast, the majority SINR in case 2 is between 15 dB and 25 dB.

This significantly different SINR distribution tells us that, even with the same public safety incident area, its location relative to the network could lead to significant performance differences. Recall that MCS used for MBSFN transmissions is selected to be the minimum MCS over all UEs. This result can provide very insightful guides to deploy mobile base stations when public safety incidents are out-of-coverage of macro-cells. For instance, with the same incident area size and shape, if first responders are concentrated within a small area, deploying mobile base stations as in case 1 would lead to much higher MBSFN MCS applied. In contrast, if first responders are evenly located across a relatively large area, mobile base station deployments based on case 2 is preferred to achieve higher MBSFN MCS since minimum MCS of all UEs can achieve relatively good value.

The next set of cases consists of three sites or nine cells as the MBSFN area. In case 3, three sites are deployed along a line, as shown in Figure 16a, and in case 4, three sites are arranged to form a triangle, as shown in Figure 18a. The SINR heatmaps in Figure 16b and Figure 18b, together with their CDFs in Figure 17 and Figure 19, show that the cells in case 3 share similar SINR distribution, whereas the cells in case 4 are more dispersed with Cell 1, 6, and 8 having better SINR over other cells. This is reasonable since they are located closer to the ‘center’ of the MBSFN area and experiencing higher

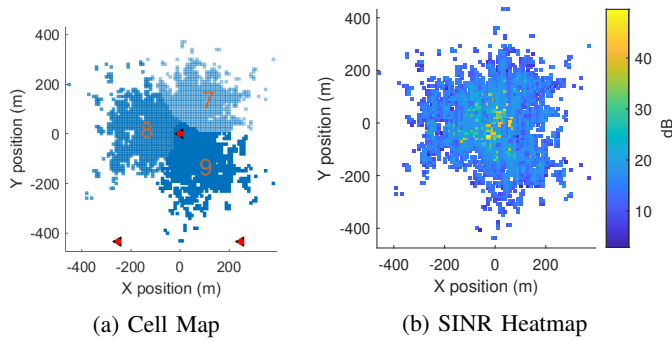


Fig. 12: MBSFN 3-cell Map, Case 1

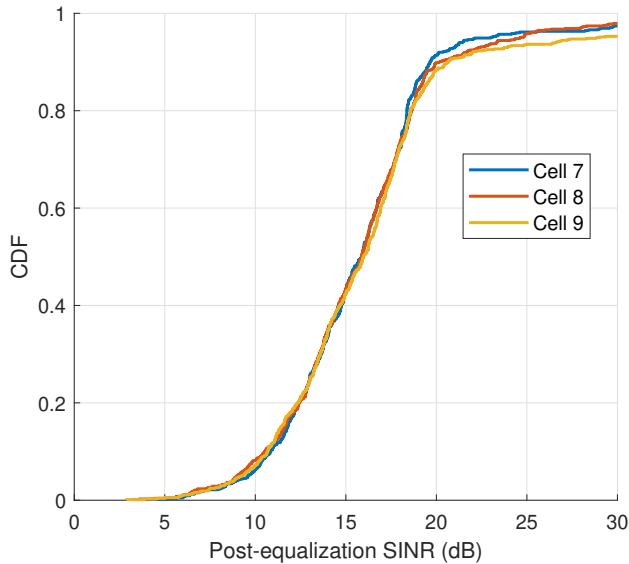


Fig. 13: MBSFN 3-cell CDF, Case 1

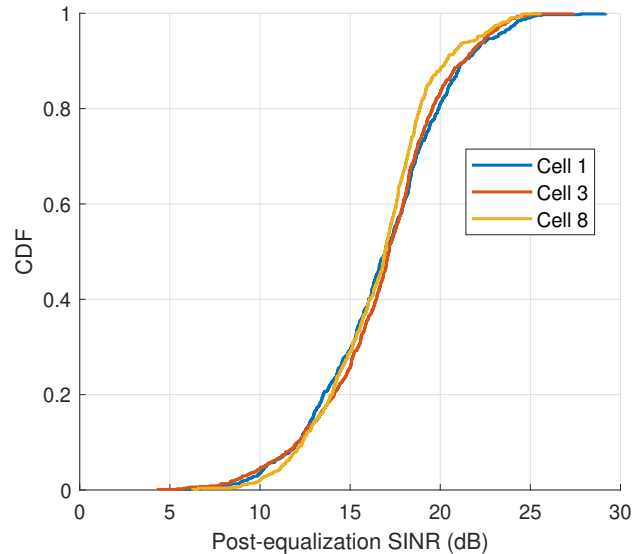


Fig. 15: MBSFN 3-cell CDF, Case 2

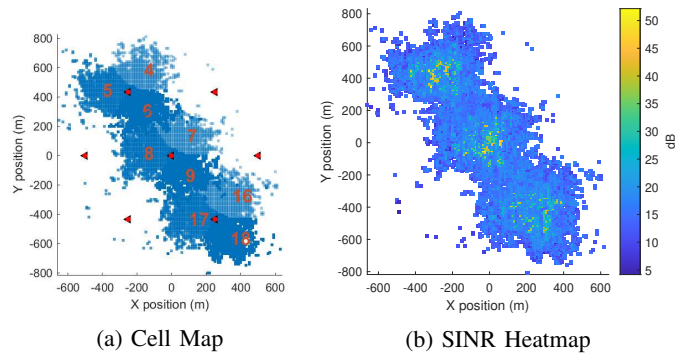


Fig. 16: MBSFN 3-site Map, Case 3

MBSFN gain, especially the portion coming from interference reduction. Unlike the case set with three cells where both cases are advantageous when serving some specific conditions, in this scenario, case 4 outperforms case 3 comprehensively.

This result tells us that even if public safety incidents cover the same area size, their different area shapes will lead to different performances. Note that by comparing SINR CDFs

with MBSFN area size of 3, 9, or 21 cells shown earlier, we can see that different MBSFN area sizes lead to a different performance, too, with more considerable SINR improvement with larger area size.

To sum up, the simulation results in this section can be directly used to predict and evaluate performance when there exists an underlying macro-cell network in the public safety incident area. When the incident is out-of-coverage of macro-cell networks, the results can be used to guide mobile base station deployments.

IV. CONCLUSION

In this paper, we have investigated UE post-equalization SINRs across MBSFN area with different area sizes and shapes. With the introduction of the multicast mechanism, we first showed the different patterns of wide-band signal and interference in MBSFN versus unicast, where the wide-band interference of the 21-cell MBSFN area forms a concentric scheme with the lowest interference at the center. We then compared the selected cells from unicast and 21-cell MBSFN, where the post-equalization SINR improves dramatically in MBSFN while showing distinct distributions among cells,

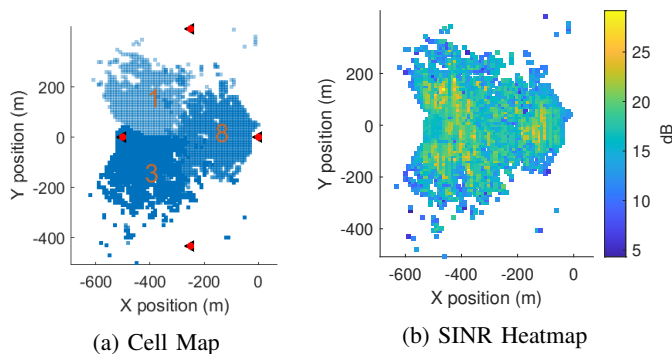


Fig. 14: MBSFN 3-cell Map, Case 2

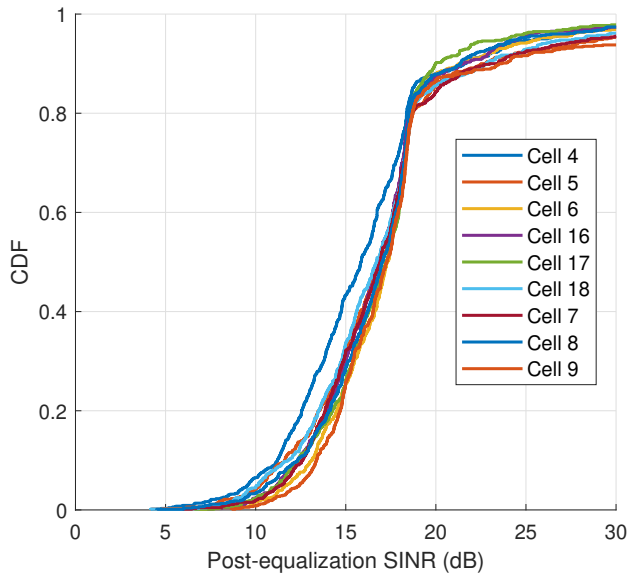


Fig. 17: MBSFN 3-site CDF, Case 3

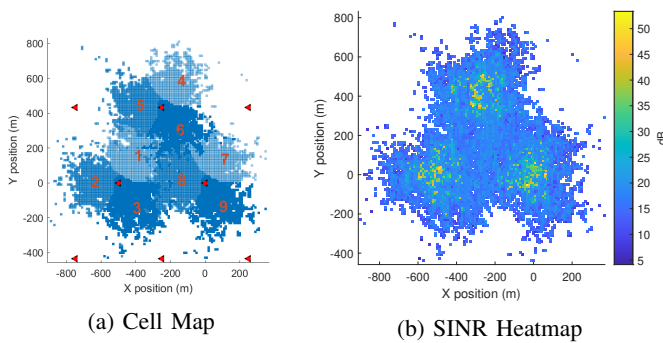


Fig. 18: MBSFN 3-site Map, Case 4

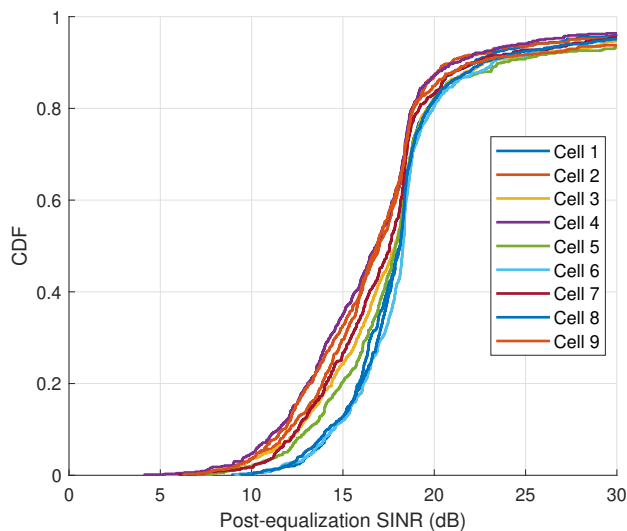


Fig. 19: MBSFN 3-site CDF, Case 4

area shapes with the same number of MBSFN cells, 3-cells and 9-cells over 3-sites, respectively. We showed that not only MBSFN area size impacts performance, but also MBSFN area shape and its relative locations to the network. The results obtained can provide insightful assessments for real case MBSFN performance and guides for mobile base station deployments in case of out-of-coverage.

REFERENCES

- [1] 3GPP TS23.246, "Multimedia Broadcast/Multicast Service (MBMS) Architecture and Functional Description," 3GPP, Standard, 9 2019.
- [2] 3GPP TS25.346, "Technical Specification group radio access network; introduction of the multimedia broadcast multicast service (MBMS) in the radio access network (RAN); stage 2 (release 9)," 3GPP, Standard, 9 2009.
- [3] K. Kirev and S. Schwarz, "Investigation of optimal mcs and subcarrier spacing in mbsfn systems," in *WSA 2020; 24th International ITG Workshop on Smart Antennas*, 2020, pp. 1–6.
- [4] L. Zhang, Y. Cai, Z. He, C. Wang, and P. Skov, "Performance evaluation of lte mbms baseline," in *2009 5th International Conference on Wireless Communications, Networking and Mobile Computing*, 2009, pp. 1–4.
- [5] 3GPP TS36.101, "Evolved Universal Terrestrial Radio Access (E-UTRA); user equipment (ue) radio transmission and reception," 3GPP, Standard, 6 2020.
- [6] A. Alexiou, C. Bouras, V. Kokkinos, A. Papazois, and G. Tschritzis, "Efficient mcs selection for mbsfn transmissions over lte networks," in *2010 IFIP Wireless Days*, 2010, pp. 1–5.
- [7] 3GPP TS36.213, "Evolved Universal Terrestrial Radio Access (E-UTRA); Physical Layer Procedures," 3GPP, Standard, Jan. 2019.
- [8] C. Liu, C. Shen, J. Chuang, R. A. Rouil, and H. Choi, "Evaluating unicast and mbsfn in public safety networks," in *IEEE PIMRC 2020 - 2020 IEEE International Conference on Communications*, Aug. 2020.
- [9] C. Borgiattino, C. Casetti, C. Chiasserini, and F. Malandrino, "Efficient area formation for lte broadcasting," in *2015 12th Annual IEEE International Conference on Sensing, Communication, and Networking (SECON)*, 2015, pp. 202–210.
- [10] C. Shen, M. Yun, A. Arora, and H.-A. Choi, *Efficient Mobile Base Station Placement for First Responders in Public Safety Networks*, 01 2020, pp. 634–644.
- [11] C. Shen, M. Yun, A. Arora, and H. Choi, *Dynamic Placement Algorithm for Multiple Classes of Mobile Base Stations in Public Safety Networks*, 08 2019, pp. 112–125.
- [12] Z. Hanzaz and H. D. Schotten, "Analysis of effective sinr mapping models for mimo ofdm in lte system," in *2013 9th International Wireless Communications and Mobile Computing Conference (IWCMC)*, 2013, pp. 1509–1515.
- [13] C. Liu, C. Shen, J. Chuang, A. R. Rouil, and H. Choi, "Throughput Analysis between Unicast and MBSFN from Link Level to System Level," in *IEEE 90th Vehicular Technology Conference*, September 2019.

which further confirms the previous wide-band observations. Moreover, we explored different deployment locations and